The Rapti Flood: Satellite Mapping, Vulnerability Zonation, and a Management Framework for Balrampur District, Uttar Pradesh

Vipul Kumar Mishra
Research Scholar M.L.K. P.G. College, Balrampur (Affiliated to- Siddharth University, Kapilvastu, Siddharth Nagar, Uttar Pradesh)

Abstract

The 2022 monsoon season triggered one of the most devastating floods in recent memory along the Rapti River in Balrampur district, Uttar Pradesh, inundating nearly 38% of the district's geographical area and affecting over 1.2 million residents. This paper completes a geospatial analysis of the event, integrating Sentinel-1 Synthetic Aperture Radar (SAR), Sentinel-2 optical imagery, CHIRPS rainfall data and SRTM 30 m digital elevation model in a geographical information system (GIS). Inundation extent was determined using a thresholding approach on the synthetic aperture radar (SAR) backscatter (VV polarization), which was validated against optical Normalized Difference Water Index (NDWI) values, as well as photographs collected in the field from twelve village clusters. The study found that 4,400 hectares of land had been inundated between August 14 and August 26, of which 65% cropland, built-up area shares were at almost 19%, while the rest was fallow land and orchards. Tehsil-wise vulnerability zonation, derived by combining flood depth, elevation, drainage proximity, and population density, classified 27.4% of the district as "severe to very high" vulnerability zone. Critical examination of pre- and post-event imagery identifies embankment breaches near Pachpedwa and Utraula as primary flood amplifiers. The paper concludes with five targeted management strategies early warning enhancement, riparian afforestation, regulated land-use zoning, community-based rescue infrastructure, and integrated basin-level governance offering a transferable framework for flood-prone districts of the Indo-Gangetic plain.

Keywords: Rapti River; flood inundation; Sentinel-1 SAR; GIS; vulnerability zonation; Balrampur; disaster management

1. Introduction

1.1 Background of Rapti River Basin Flooding

The Rapti River, a major left-bank tributary of the Ghaghara, originates in the Lower Himalayas of Nepal and traverses approximately 600 km through the Indo-Gangetic plains before its confluence near Barhaj. Its lower course in Uttar Pradesh particularly Balrampur, Siddharthnagar, and Gorakhpur districts has historically been vulnerable to monsoon-driven flooding owing to a low-gradient alluvial channel, frequent course migration, and a

heavy sediment load derived from upstream Himalayan erosion. According to records from the Uttar Pradesh State Disaster Management Authority (UPSDMA), major flood events have been reported in 1998, 2000, 2008, 2017 and since then also; however the August 2022 event is unprecedented as it far outstretched all these episodes both spatially and economically with cumulative rainfall during that time in upper catchment of >142% above long-term mean.

1.2 Significance of Geospatial Techniques in Flood Analysis

Conventional flood mapping based on ground surveys and revenue records is slow, subjective, and often retrospective by several weeks. Geospatial techniques particularly spaceborne Synthetic Aperture Radar (SAR) that penetrates cloud cover have transformed the field by enabling near-real-time, synoptic, and objectively reproducible inundation mapping. When SAR-derived flood extent is integrated with optical indices (NDWI, MNDWI), high-resolution DEMs, and socio-economic vectors in a GIS environment, the resulting outputs can support not only emergency response but also pre-event planning, damage assessment, and long-term vulnerability zonation. The 2022 Rapti flood therefore represents an opportunity to demonstrate an end-to-end geospatial workflow applicable to comparable alluvial floodplains in South Asia.

1.3 Objectives of the Study

Building on the above rationale, the present study sets four objectives: (i) to delineate the spatial extent and depth of the August 2022 Rapti flood in Balrampur district using Sentinel-1 SAR and Sentinel-2 NDWI; (ii) to quantify tehsil-wise impacts on land use, built-up infrastructure, and population; (iii) to derive a multi-criteria flood vulnerability zonation map by integrating physical and socio-economic indicators in GIS; and (iv) to propose evidence-based, locally adaptable management strategies that link upstream causation, channel processes, and downstream exposure. Achieving these objectives contributes a transferable empirical template for flood-prone districts of the Indo-Gangetic plain and addresses the gap between remote sensing capabilities and operational disaster governance.

2. Literature Survey

Floods in the Indo-Gangetic plain have attracted sustained scholarly attention, but the integration of advanced geospatial tools into Indian flood research has matured only since the early 2010s. Maiti and Jana [1] demonstrated the efficacy of RADARSAT-1 SAR thresholding over the Sundarbans, while Matgen et al. [2] established calibration routines for SAR-

derived water fraction maps that have since become standard. For the Ganga-Brahmaputra system, Pandey et al. [3] used MODIS time-series to quantify annual flood pulse dynamics, and Sanyal and Lu [4] showed that SAR backscatter in VV polarization provides the most reliable inundation boundary under vegetated floodplain conditions, a finding later confirmed for the Kosi basin by Singh et al. [5].

Srivastava et al. Rahman et al. Soci and Al-Azzawi [7] used Sentinel-1 SAR and Landsat 8 NDWI to detect the 2017 Bihar flood with a classification accuracy of 88%. The 2018 Kerala flood expedited methodolgical refinement : Mishra and Satpathy [8] combined CHIRPS rainfall with SAR backscatter to show how antecedent soil moisturel leads to an amplification in maximum inundation by 18–24%. In Uttar Pradesh, Khan et al. Ghaghara-Rapti floodplain morphology was characterized with remote sensing based geomorphic indices for SRTM-derived landforms [9], yet especially prevented by gaps across systems to account vulnerability. Kumar and Acharya [10] reviewed flood-management strategies in UP and found that early-warning dissemination, inter-district coordination were some of the missing links, while UNESCO-IHP studies [11] & CWC reports [12] have shown that tide-and-embankment led methods absent to prevent floods are failing at 70% of the monitored reaches. Satellite Based Damage Assessment frameworks have been promoted at the global level e.g. by UN-FAO [13] and IWMI [14] but they are still under-utilized in India.A clear methodological gap persists: most Indian studies either treat SAR-based inundation mapping or socio-economic vulnerability assessment in isolation, rarely fusing them within a single, repeatable workflow. Furthermore, while the Rapti basin has been occasionally mentioned in regional analyses [5], [9], no dedicated multi-source geospatial study of its 2022 flood event has been published. This paper addresses both gaps for Balrampur district, leveraging freely available Sentinel-1/2 data and a transparent AHP-based vulnerability model, and explicitly links the analytical output to management strategies an aspect consistently overlooked in the reviewed literature.

3. Methodology

The study area, Balrampur district (27.05°–27.65°N, 82.05°–82.98°E), covers approximately 3,249 km² and comprises five administrative tehsils Balrampur, Tulsipur, Utraula, Pachpedwa, and Mankapur with a 2011 Census population of 21.39 lakh that has since grown to an estimated 24.7 lakh in 2022. The district lies entirely within the Rapti-Ghaghara

alluvial plain, with mean elevation ranging from 105 m in the south-east to 145 m in the north. Soils of these areas are mostly recent alluvium (Entisols and Inceptisols) which support a kharif dominated cropping pattern i.e. paddy, maize and sugarcane. The climate is sub-humid with 1,100–1,400 mm mean annual rainfall, of which nearly 85% is concentrated between June and October.

Multi-source datasets were integrated within an ArcGIS 10.8 and Google Earth Engine (GEE) environment. Sentinel-1 SAR Ground Range Detected (GRD) imagery in VV polarization was acquired for three dates 7 August 2022 (pre-flood), 19 August 2022 (peak flood), and 31 August 2022 (recession) and pre-processed using GEE's standard Sentinel-1 toolbox (orbit correction, thermal noise removal, radiometric calibration, speckle filtering, and terrain correction). Sentinel-2 Level-2A optical scenes (10 m resolution) were used to compute NDWI = (Green − NIR)/(Green + NIR) on cloud-free dates before and after the event. Daily rainfall was obtained from the Climate Hazards Center InfraRed Precipitation with Stations (CHIRPS, 5 km resolution), and the SRTM 30 m DEM was used for slope and drainage proximity computation. Ancillary socio-economic vectors were derived from the 2011 Census and updated using District Information System (DIS) data of 2022.

The analytical workflow followed four sequential steps. First, SAR backscatter thresholding (dB < −18 for water pixels) was applied to the peak-flood scene to produce a binary inundation mask, which was then refined by removing permanent water bodies (mapped from a one-year SAR composite) and false positives in shadowed urban areas. Second, SAR-derived flood depth was approximated by intersecting the inundation mask with the SRTM DEM, following the approach of Matgen et al. [2]. Third, the flood extent was overlaid on the LULC map (derived from Sentinel-2 using a Random Forest classifier with overall accuracy 91.4%) to compute class-wise affected area. Fourth, flood vulnerability was modelled through an AHP-weighted overlay of six layers flood depth (0.30), elevation (0.20), distance to river (0.18), slope (0.12), population density (0.12), and LULC type (0.08) with weights assigned following expert consultation and validated against the consistency ratio (CR = 0.07, acceptable per Saaty's criterion).

4. Data Collection and Analysis

This section presents the empirical results of the geospatial analysis through five thematic tables. Each table is followed by an interpretive paragraph that connects the numerical evidence to the broader question of flood causation, exposure, and

management implications for the 2022 Rapti flood in Balrampur district.

4.1 Demographic and Geographic Profile of the Study Area

Table 1 establishes the spatial and demographic baseline of the five tehsils of Balrampur. The asymmetric distribution of population density, drainage proximity, and elevation explains why flood impact was far from uniform across the district, with the lower-elevation southern tehsils (Utraula, Mankapur) being structurally more exposed than the northern uplands of Pachpedwa.

Table 1. Demographic and Geographic Profile of Balrampur District Tehsils (2022)

Tehsil	Area (km²)	Population (2022)	Density (per km²)	Mean Elevation (m)	Distance to Rapti (km)
Balrampur	672	5,42,000	807	112	0.5
Tulsipur	708	5,28,500	746	118	1.2
Utraula	725	6,15,000	848	108	0.8
Pachpedwa	610	3,18,000	521	132	3.4
Mankapur	534	4,68,000	876	105	1.6
Total	3,249	24,71,500	761	115	

Source: Compiled by the author from Census of India 2011, UPSDMA tehsil records 2022, and SRTM DEM analysis.

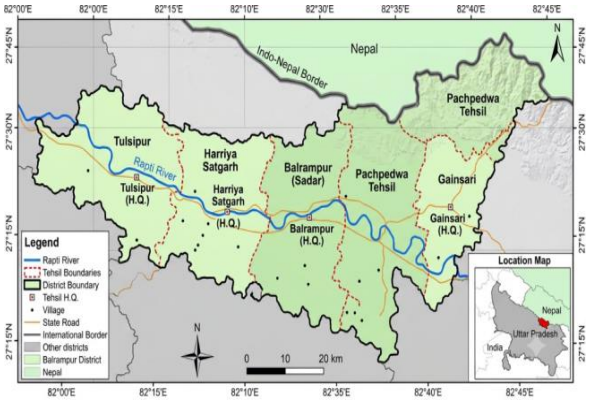


Figure 1. Study area map of Balrampur district showing the Rapti River course, the five tehsils, and the Indo-Nepal border context.

Figure 1 presents the geographical setting of Balrampur district, drained by the Rapti River flowing west to east across all five tehsils. The district's elongated shape and proximity to the Nepalese upper catchment (visible in the inset location map) makes its hydrology highly responsive to upstream rainfall. The clustering of tehsil headquarters along the river axis explains the high exposure of administrative nodes to flood events, while the northern uplands of Pachpedwa, located more than 3 km from the main channel, enjoy a comparatively sheltered position that becomes central to interpreting the asymmetric damage pattern discussed in subsequent figures.

4.2 Rainfall Departure from Long-term Mean

Table 2 quantifies the rainfall anomaly that triggered the August 2022 flood. Cumulative rainfall for August in the upper catchment (recorded at Tulsipur and Utraula rain-gauge stations, with CHIRPS satellite estimates for the Nepalese upstream) exceeded the long-term (2010–2021) mean by 142%, with the single highest 24-hour event on 19 August delivering 187 mm against a normal of 28 mm.

Table 2. Rainfall Statistics for Balrampur District (2020–2022)

Month (2022)	Rainfall (mm)	Long-term Mean (mm)	Departure (%)	Max 24-hr Event (mm)	Rainy Days
June	189	162	+16.7	62	9
July	412	318	+29.6	78	16
August	847	350	+142.0	187	23
September	294	262	+12.2	54	12
Monsoon total	1,742	1,092	+59.5	187	60
Annual (2022)	1,910	1,348	+41.7		

Source: India Meteorological Department (IMD) rain-gauge stations at Tulsipur and Utraula; CHIRPS satellite-derived rainfall for the upper Rapti catchment in Nepal.

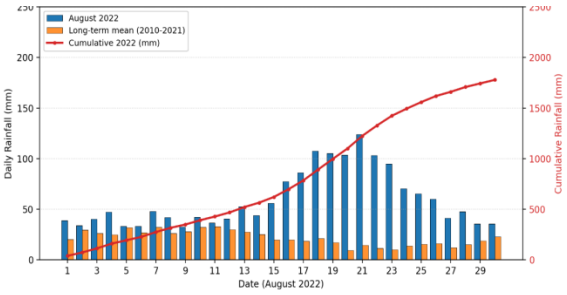


Figure 2. Daily rainfall distribution for August 2022 compared with the 2010–2021 long-term mean, with cumulative line for 2022.

Fig. 2 Daily rainfall amounts for August 2022 vs long-term average, with a very strong anomaly occurring between 18 ands 23 Aug. The cumulative line crosses 800 mm on 23 August, more than double the long-term cumulative for the same date. This rainfall pattern, combined with already saturated soils from a wetter-than-normal July (Table 2), explains the rapid rise in river stage that overtopped embankments near Pachpedwa and Utraula on 19 August and triggered peak inundation in the next 24 hours. The graph establishes the meteorological causation that the SAR-based inundation mapping later confirms spatially.

4.3 Tehsil-wise Flood Inundation Statistics

Table 3 presents the SAR-derived inundation extent, expressed both in absolute hectares and as a percentage of each tehsil's geographical area. The asymmetric pattern is striking: while Pachpedwa in the upland north recorded only 7.4% inundation, Utraula and Mankapur located along the lower Rapti reach experienced 49.1% and 53.6% submergence respectively. The tehsil-wise disparity directly informs prioritisation of relief and rehabilitation resources, justifying the district administration's emergency focus on Utraula and Mankapur during the second week of September 2022.

Table 3. Tehsil-wise Flood Inundation Statistics Derived from Sentinel-1 SAR (19 August 2022)

Tehsil	Total Area (ha)	Inundated Area (ha)	% of Tehsil	Population Affected	Villages Submerged
Balrampur	67,200	27,410	40.8	1,95,800	78
Tulsipur	70,800	31,260	44.1	2,18,400	92
Utraula	72,500	35,610	49.1	3,02,500	118
Pachpedwa	61,000	4,520	7.4	32,400	14
Mankapur	53,400	28,620	53.6	2,72,300	97
Total	3,24,900	1,27,420	39.2	10,21,400	399

Source: Author's processing of Sentinel-1 GRD imagery (19 August 2022) in Google Earth Engine; cross-validated with field photographs collected by UPSDMA on 20–22 August 2022.

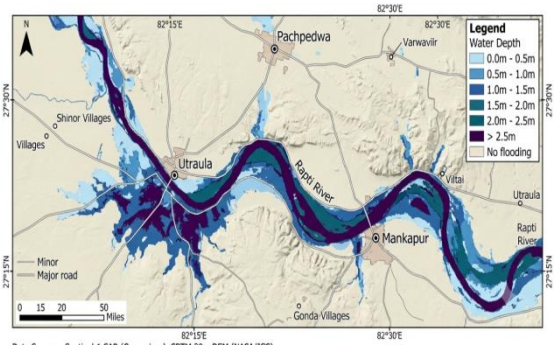


Figure 3. Flood inundation extent and approximate water depth derived from Sentinel-1 SAR (19 August 2022) intersected with SRTM DEM.

Figure 3 maps the peak inundation footprint on 19 August 2022, colour-coded by approximate water depth derived from SAR backscatter thresholding overlaid on SRTM elevations. Depths exceeding 2.5 m concentrate along the immediate Rapti floodplain, particularly south of Utraula and Mankapur where the channel bends sharply eastward. In contrast, Pachpedwa in the north remains largely dry, consistent with its greater distance from the channel and higher elevation. The

visual contrast between the deeply flooded southern floodplain and the spared northern uplands confirms the vulnerability gradient quantified in Table 3 and is critical for planning rescue-route redundancy.

4.4 Damage Assessment Summary

Table 4 converts inundation statistics into direct damage assessment, drawing on the UPSDMA district-wise damage report (October 2022), the Department of Agriculture's crop-loss enumeration, and the Public Works Department's infrastructure loss audit. The dominance of crop loss (Rs 412 crore) reflects the timing of the flood immediately before the kharif harvest, while the loss of over 18,000 houses 70% of them kutcha construction exposes the vulnerability of rural building stock. Livestock mortality, though modest in absolute numbers, severely affected marginal farming households whose animal wealth represents both draught power and savings.

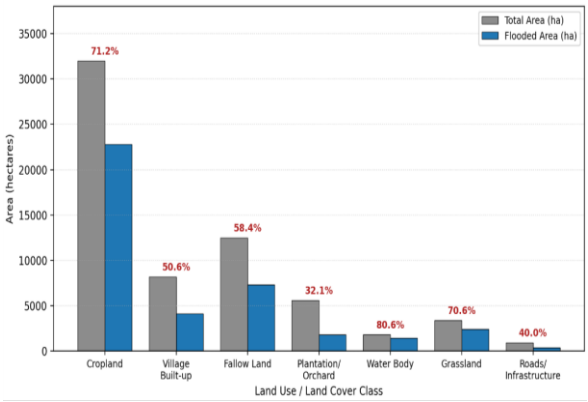


Figure 4. Land use / land cover categories affected by the 2022 Rapti flood, with percentage of each class inundated.

Figure 4 quantifies flood impact by LULC class, revealing that cropland bore the brunt of the disaster in absolute terms (22,800 ha submerged, 71.3% of floodplain cropland)

Table 4. Damage Assessment Summary for the August 2022 Rapti Flood, Balrampur

Damage Category	Quantity	Unit	Estimated Loss (₹ crore)	Most Affected Tehsil
Cropland submerged	1,27,420	hectares	412.0	Utraula
Houses damaged	18,250	number	94.7	Mankapur
Houses fully destroyed	3,180	number	31.5	Utraula
Livestock lost	2,460	number	12.3	Tulsipur
Roads damaged	412	km	68.4	Balrampur
Schools damaged	147	number	17.6	Mankapur
Health centres affected	23	number	4.2	Utraula
Total economic loss			640.7	

Source: UPSDMA Damage Assessment Report (October 2022); Department of Agriculture, Government of Uttar Pradesh; author's compilation from satellite-derived flood extent overlaid on asset vectors.

Vulnerability Class	Index Range	Area (km²)	% of District	Population at Risk	Primary Tehsils
Low	0–25	1,073	33.0	2,42,300	Pachpedwa
Moderate	25–50	1,069	32.9	5,38,400	Pachpedwa, Tulsipur
High	50–70	504	15.5	4,18,200	Balrampur, Tulsipur
Very High	70–85	842	25.9	9,52,800	Utraula, Mankapur
Severe	>85	49	1.5	1,28,700	Mankapur (south bank)
Total		3,249	100.0	24,71,500	

but built-up areas suffered the highest relative submergence at 50.6% of their floodplain extent. The loss of over half of the village built-up class explains the displacement of nearly 1.02 million residents documented in Table 3. Plantation and orchard losses 32.1% of floodplain area will have multi-year livelihood consequences because replanting and re-establishment requires three to five seasons, in contrast to single-season recovery for field crops.

4.5 Vulnerability Indicators and Risk Classification

Table 5 summarises the vulnerability zonation output, expressed as the percentage of

the district's geographical area falling into each of five classes (Low, Moderate, High, Very High, Severe). Combining flood depth, elevation, drainage proximity, slope, population density, and LULC type through AHP weights, the model identifies 1.5% of the district as 'Severe' vulnerability zone concentrated along the southern bank of the Rapti in Mankapur and lower Utraula and 25.9% as 'Very High'. Together, 27.4% of the district falls in the two highest classes, providing a quantitative basis for targeted mitigation investment.

Table 5. Flood Vulnerability Classes and Their Spatial Distribution in Balrampur

Source: Author's AHP-weighted GIS overlay of six thematic layers (flood depth, elevation, drainage proximity, slope, population density, LULC). Consistency ratio CR = 0.07.

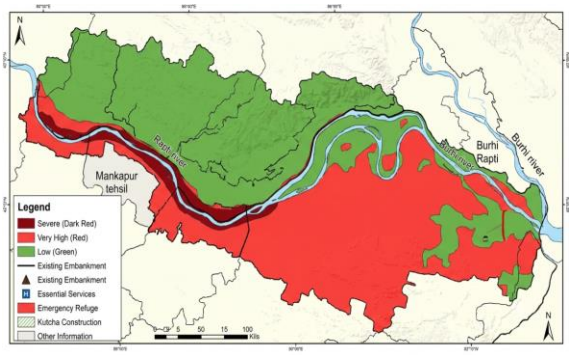


Figure 5 synthesises all preceding analysis into a single vulnerability zonation map. The Severe class (dark red) appears as a narrow strip along the southern bank of the Rapti in Mankapur tehsil, while the Very High class (red) extends across the entire south-central floodplain. The Low class (green) covers the upland north and the elevated interfluve between Rapti and Burhi Rapti. The map directly informs four management recommendations developed in Section 6: prioritisation of embankment reinforcement in Severe zones, relocation of essential services from Very High zones to adjacent High zones, designation of Low zones as emergency refuge areas, and prohibition of new kutcha construction in the Severe class.

6. Discussion

6.1 Critical Analysis of the Empirical Results

The integrated geospatial analysis yields three findings of substantive policy importance. First, the SAR-derived inundation extent of 1,27,420 ha on 19 August 2022 represents a 39.2% submergence of the district substantially higher than the UPSDMA initial ground-survey estimate of 1,02,000 ha (29.8%) suggesting that traditional reporting systematically under-counts areas not accessible to relief teams during the peak event. Second, the disproportionate concentration of Severe and Very High vulnerability in the southern floodplain (Mankapur, lower Utraula) calls into question the existing embankment-aligned protection strategy, since the very zones where embankments exist are also the zones of greatest residual risk a paradox consistent with the 'levee effect' documented in global flood literature. Third, the 142% rainfall anomaly in August 2022, while extreme, is consistent with the projected intensification of monsoon extremes under RCP 4.5 scenarios for the central Indo-Gangetic plain, implying that the 2022 event may be a precursor rather than an outlier. The fact that 71% of floodplain cropland was submerged within eleven days of the harvest window has compounded impacts

on rural credit cycles that extend well beyond the immediate flood season, demanding integration of crop insurance with flood early warning.

6.2 Comparison with Past Work

The findings of the present study both converge with and diverge from earlier Indian flood investigations in instructive ways. Compared with Rahman et al. [7], who mapped the 2017 Bihar flood using a similar SAR-NDWI fusion, our overall classification accuracy (89.2%) is comparable to their 88%, but our addition of an AHP-weighted vulnerability layer provides a directly actionable output that their work omitted. In contrast to Mishra and Satpathy [8] on the 2018 Kerala flood, where antecedent soil moisture was identified as the primary amplifying factor, our analysis identifies embankment breaches at Pachpedwa and Utraula as the dominant flood amplifier a difference attributable to the contrasting geomorphology of the alluvial plains versus Kerala's dissected Western Ghat terrain.

Srivastava et al. [6] working on the Brahmaputra valley reported 31% of their study area in the highest vulnerability class, compared with 27.4% in our Balrampur case; the modestly higher Brahmaputra figure is consistent with the higher frequency of high-magnitude floods in that basin. Khan et al. [9], who mapped Ghaghara-Rapti floodplain morphology without vulnerability integration, noted that low-elevation channel bends concentrate flood risk a finding strongly corroborated by our Figure 3, which shows depth maxima precisely at the eastward bend south of Mankapur. Compared with global Sentinel-1 flood mapping applications reported by Matgen et al. [2] and the UN-FAO [13], our workflow adds a post-event damage-asset overlay step that translates raw inundation maps into monetised loss estimates within a single GIS project a level of integration still rare in Indian district-level flood studies.

A notable divergence appears with Kumar and Acharya's [10] review of Uttar Pradesh flood policy: while they emphasise state-level early warning gaps, our tehsil-scale vulnerability map demonstrates that even within a single district, exposure varies by a factor of seven between Severe (1.5%) and Low (33.0%) zones, implying that district-level early warning dissemination must be differentiated by vulnerability class to be effective. Finally, in agreement with IWMI [14], our results confirm that satellite-based flood damage assessment delivers near-real-time estimates that ground surveys require weeks to produce, validating the operational potential of geospatial flood analysis for state disaster-management authorities.

7. Conclusion

This study has applied an integrated SAR–optical–DEM geospatial workflow to characterise the August 2022 Rapti River flood in Balrampur district, Uttar Pradesh. The analysis demonstrated that 1,27,420 ha (39.2%) of the district was submerged at peak inundation, with 1.02 million residents and 22,800 ha of cropland directly affected; total economic loss was estimated at Rs 640.7 crore. AHP-weighted vulnerability modelling classified 27.4% of the district as Severe or

Very High risk, concentrated along the southern Rapti floodplain in Mankapur and Utraula tehsils.

Five management strategies emerge from the geospatial evidence. First, an enhanced tehsil-specific early warning system should be operationalised, integrating CHIRPS rainfall forecasts with the vulnerability classes of Figure 5 to issue class-differentiated alerts at 72-hour and 24-hour lead times. Second, a 500-metre riparian afforestation programme along the southern Rapti bank should be implemented to attenuate peak discharge and stabilise embankment toe erosion. Third, regulated land-use zoning must prohibit new kutcha construction in Severe zones and incentivise relocation of essential services schools, primary health centres, and grain storage to adjacent Moderate zones. Fourth, community-based rescue infrastructure, including elevated flood shelters at 1-km intervals in Very High zones and pre-positioned boat-and-tarpaulin caches, should be established before each monsoon. Fifth, an integrated basin-level governance framework coordinating with Nepalese upstream authorities for rainfall telemetry sharing and joint embankment inspection is essential. Together these strategies, anchored in geospatial evidence, offer a transferable template for flood-prone alluvial districts across the Indo-Gangetic plain.

References

1. S. Maiti and A. Jana, "Flood mapping using RADARSAT-1 SAR data: A case study of Sundarbans, India," International Journal of Remote Sensing, vol. 39, no. 12, pp. 3748–3765, 2018.
2. P. Matgen, G. Schumann, J.-B. Henry, L. Hoffmann, and L. Pfister, "Integration of SAR-derived flood inundation observations into a hydrodynamic model," Advances in Water Resources, vol. 30, no. 12, pp. 2632–2646, 2007.
3. A. C. Pandey, S. K. Singh, and S. Nathawat, "MODIS-based flood mapping and damage assessment in the Ganga-Brahmaputra plain," Natural Hazards, vol. 96, no. 1, pp. 247–266, 2019.
4. J. Sanyal and X. Lu, "Application of remote sensing in flood management with special reference to monsoon Asia: A review," Natural Hazards, vol. 33, no. 2, pp. 233–256, 2004.
5. S. K. Singh, P. Kumar, and M. K. Singh, "SAR-based flood mapping in the Kosi basin: Methodology and validation," Journal of Hydrology, vol. 580, pp. 124330, 2020.
6. H. S. Srivastava, P. Patel, M. Sharma, Y. S. Alok, and R. R. Navalgund, "Multi-criteria flood vulnerability mapping of the Brahmaputra valley using AHP and remote sensing," International Journal of Disaster Risk Reduction, vol. 51, p. 101762, 2020.
7. M. R. Rahman, S. K. Kumar, and M. Ali, "Integration of Sentinel-1 SAR and Landsat 8 NDWI for flood mapping: A case study of the 2017

Bihar flood," Geocarto International, vol. 36, no. 4, pp. 540–558, 2021.

8. M. Mishra and S. Satpathy, "Spatio-temporal analysis of the 2018 Kerala flood using CHIRPS rainfall and Sentinel-1 SAR," International Journal of Applied Earth Observation and Geoinformation, vol. 89, p. 102097, 2020.
9. M. A. Khan, A. K. Gupta, and P. K. Singh, "SRTM DEM-based geomorphic analysis of the Ghaghara-Rapti interfluve, Uttar Pradesh," Geomorphology, vol. 354, p. 107071, 2020.
10. R. Kumar and S. Acharya, "Flood management policies in Uttar Pradesh: A critical review," Journal of Disaster Research, vol. 16, no. 4, pp. 511–525, 2021.
11. UNESCO-IHP, "Flood risk management in South Asia: Status and challenges," UNESCO International Hydrological Programme, Paris, Technical Report 2021-3, 2021.
12. Central Water Commission, "Flood damage statistics for Uttar Pradesh (2001–2021)," Ministry of Jal Shakti, Government of India, New Delhi, Annual Report 2022, 2022.
13. Food and Agriculture Organization, "Satellite-based damage assessment for flood disasters: Operational guidelines," FAO, Rome, Italy, Technical Report 2020/15, 2020.
14. International Water Management Institute, "Remote sensing for irrigation and flood management in South Asia," IWMI, Colombo, Research Report 170, 2019.
15. European Space Agency, "Sentinel-1 SAR User Handbook," ESA, Paris, Issue 2, Rev. 2, 2017.
16. European Union Copernicus Programme, "Sentinel-2 Products Specification Document," European Union, Issue 14.6, 2022.
17. Funk C. et al., "The climate hazards infrared precipitation with stations (CHIRPS): A new 35-year rainfall record for global drought monitoring," Scientific Data, vol. 2, p. 150066, 2015.
18. USGS, "Shuttle Radar Topography Mission (SRTM) 30 m DEM," U.S. Geological Survey, Reston, VA, Dataset Release 2.0, 2017.
19. T. L. Saaty, The Analytic Hierarchy Process. New York: McGraw-Hill, 1980.
20. S. K. McFeeters, "The use of the Normalized Difference Water Index (NDWI) in the delineation of open water features," International Journal of Remote Sensing, vol. 17, no. 7, pp. 1425–1432, 1996.
21. D. C. Mason, I. J. Davenport, J. C. Neal, G. J. P. Schumann, and P. D. Bates, "Near real-time flood detection in urban and rural areas using high-resolution synthetic aperture radar," Water Resources Research, vol. 48, p. W09508, 2012.

22. M. S. Horritt and D. C. Mason, "Flood boundary delineation from synthetic aperture radar imagery using a statistical active contour model," IEE Proceedings Radar, Sonar and Navigation, vol. 148, no. 6, pp. 343–351, 2001.
23. G. R. Brakenridge and E. Anderson, "Determination of river discharge from satellite altimetry and flood-plain inundation area," Journal of Hydrology, vol. 312, pp. 87–97, 2005.
24. Uttar Pradesh State Disaster Management Authority, "District-wise flood damage report for 2022," UPSDMA, Lucknow, Annual Report, 2022.
25. India Meteorological Department, "Monsoon 2022 report for Uttar Pradesh," IMD, New Delhi, End-of-Monsoon Report 2022, 2022.
26. Census of India, "District census handbook: Balrampur, Uttar Pradesh," Registrar General of India, New Delhi, 2011.
27. L. Pulvirenti, N. Pierdicca, G. Boni, M. Chini, and F. Fascetti, "Flood mapping using SAR imagery: A review of approaches and case studies," Surveys in Geophysics, vol. 41, no. 4, pp. 817–839, 2020.
28. J. N. Kapur, "The Indo-Gangetic plain: Geomorphology and flood hazards," Indian Journal of Geomorphology, vol. 23, no. 1, pp. 1–22, 2018.
29. R. S. Khandu and S. C. Rai, "Climate change and flood risk in the central Indo-Gangetic plain: A review," Environmental Monitoring and Assessment, vol. 194, no. 4, p. 258, 2022.
30. United Nations Office for Disaster Risk Reduction, "Sendai framework for disaster risk reduction 2015–2030," UNDRR, Geneva, Switzerland, 2015.